C. R. Chimie 18 (2015) 668–677

Contents lists available at ScienceDirect

Comptes Rendus Chimie

www.sciencedirect.com

Full paper/Mémoire

Influence of basil oil extract on the antioxidant and antifungal activities of nanostructured carriers loaded with nystatin

Gabriela Badea, Alin Gabriel Bors, Ioana Lacatusu, Ovidiu Oprea, Camelia Ungureanu, Raluca Stan *, Aurelia Meghea

"Politehnica" University of Bucharest, Faculty of Applied Chemistry and Material Science, Polizu Street No. 1, 011061 Bucharest, Romania

ARTICLE INFO

Article history:
Received 8 August 2014
Accepted after revision 30 September 2014
Available online 21 March 2015

Keywords:
Basil
Nystatin
Nanostructured carriers
Antifungal action
Antioxidant activity

ABSTRACT

The combination of basil oil, natural antifungal, and nystatin has the potential to prevent the extension of topical fungal infections towards systemic infections. The aim of this study was to develop formulations based on basil oil and nystatin with the desired antifungal and antioxidant activity and low toxicity by using lipid nanocarriers. The synthesized nanocarriers showed spherical and homogeneous particles with main diameters less than 150 nm, as determined by TEM. The scanning calorimetric study revealed an imperfect crystallization in the core of lipid nanocarriers. Quantitative results suggested that basil oil concentration affects encapsulation efficiency. The prepared nanocarriers guaranteed an increased nystatin encapsulation by using 3% basil oil content. Chemiluminescence assay proved that the protective activity against oxygen free radicals was influenced by nystatin concentration. The in vitro antifungal studies revealed a better activity of the nanocarriers loaded with 1% nystatin in comparison with 0.5% loading.

© 2014 Académie des sciences. Published by Elsevier Masson SAS. All rights reserved.

1. Introduction

In recent years, despite the progress made in modern medicine, an increase in fungal infections was noticed [1,2]. The factors behind this increase include a weakened immune system, the treatment with corticosteroids and broad-spectrum antibiotics [3–5], the large number of cancers that imply a long-term chemotherapy [6], and the increased number of patients with chronic viral infections [7] and with various metabolic conditions [8,9]. The need to combat fungal infections makes the study of antifungal actives of great interest. Antifungals may be used in topical application for systemic mycoses. A fungal infection in immunosuppressed patients involves a high consumption of resources to eradicate fungi and a high risk of fatal complications [10]. Thus, a major goal is to prevent the progression of localized fungal infections towards systemic infections. This can be achieved by developing antifungal drugs with local action and minimal toxicity to the body, in order to limit and to eliminate the infections at the entrance gate [11,12]. Among antifungal drugs, the most important classes of antifungal compounds are polyenes, azole and echinocandins derivatives [13]. Many natural products, such as green tea [14], thyme [15,16], basil oil or other herbs proved to be effective in the treatment of topical fungal infections [17,18].

In this respect, two antifungals were selected in the present research to develop nanostructured lipid carriers (NLCs) able to combat fungal infections and free oxygen radicals, e.g., basil oil extract and a biosynthesized antibiotic, nystatin, produced by *Streptomyces noursei*. Nystatin belongs to the class of polyenes (Fig. 1), which

* Corresponding author.
E-mail address: rl_stan2000@yahoo.com (R. Stan).

http://dx.doi.org/10.1016/j.crci.2014.09.012
1631-0748/© 2014 Académie des sciences. Published by Elsevier Masson SAS. All rights reserved.

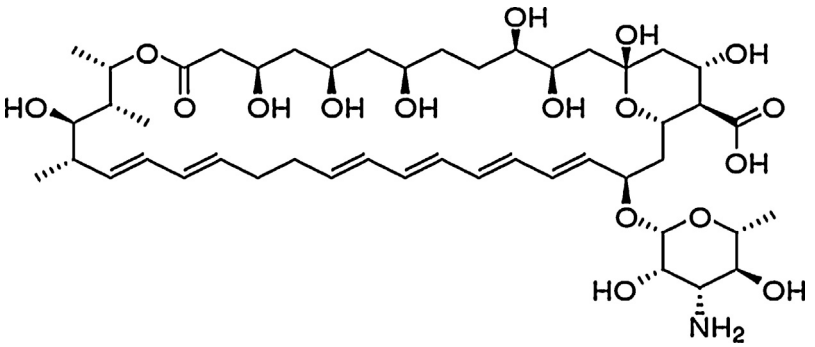

Fig. 1. Nystatin.

have been used in antifungal therapy for over 50 years, but their use is limited because of their high toxicity versus the human body [19,20]. Nystatin acts by irreversible binding to ergosterol and other specific sterols from the fungal cell membrane, leading to the formation of membrane pores through which ions are lost [13]. This leads to the destruction of the fungal cells.

Beside the antifungal action, the vegetable sources of active compounds could act as valuable natural antioxidants, and not only. The entrapment of vegetable extracts into various systems (e.g., liposome, nanostructured silica, lipid nanoparticles, etc.) has led to high fluorescent and improved antioxidant properties [21–25]. Nanostructured lipid carriers (NLC) are colloidal carrier systems composed of physiological lipid materials and surfactants accepted as GRAS [26,27] with high drug loading, encapsulation efficiency and stability [28–30] and, most importantly, they may increase bioavailability and stability of bioactive compounds and provide controlled release of encapsulated materials [31,32]. They have been accepted by regulatory authorities for application in cutaneous drug delivery (e.g., topical, dermal and transdermal) for both cosmetic and pharmaceutical areas [33,34].

The aim of this research was to synthetize lipid nanocarriers based on basil extract and loaded with Nys in order to reduce nystatin's toxicity and to increase their antifungal and antioxidant efficiency. Basil oil extract was used in this research with a dual purpose, firstly as natural antifungal and antioxidant agent, and secondly, as a component of the lipid matrix that will incorporate the antibiotic.

2. Experimental

2.1. Materials

Nystatin (Nys) was purchased from Antibiotics Iasi, Romania. Polyoxyethylene-sorbitan monooleate (Tween 80) was supplied by Merck (Germany). Synperonic PE/F68 (block copolymer of polyethylene and polypropylene glycol) and L-α-phosphatidylcholine were obtained from Sigma–Aldrich Chemie GmbH (Munich, Germany). Basil oil extract (BO) was purchased from Hofigal, Romania, and its fatty acid content has been determined by gas chromatography, using the derivatization method, which involves the transesterification of the oil with NaOH 0.5 N in methanol. Fatty acid methyl esters that were obtained after transesterification were subjected to gas-chromatographic analysis (Agilent Technologies, 7890A) coupled with mass spectrometry (Agilent Technologies, model 5975C VL MSD). The separation was performed on Supelco SP™ 2560 column (100 m, 0.25 mm internal diameter and 0.2 μm film thickness) with helium as the carrier gas (flow rate of 1.5 mL/min). The identification of the peaks was made by comparing the retention times with those of a standard mixture of 37 fatty acid methyl esters (FAME Mix Component Supelco™ 37). The fatty acids of BO were: 61.88% linoleic acid, 28.73% oleic acid, 5.60% palmitic acid, 3.45% stearic acid, 0.33% behenic acid. The solid lipids used were: *n*-hexadecyl palmitate (CP) purchased from Acros Organics (USA) and glyceryl monostearate (GMS) from Cognis GmbH.

2.2. Preparation of lipid nanoparticles

NLC were prepared using the melt emulsification coupled with high-pressure homogenization (HPH) method, according to the procedure described elsewhere [35]. Briefly, the aqueous phase containing a 2.5% surfactant mixture was heated under stirring at 85 °C. The lipid phase consisting of CP, GMS and BO was heated under stirring at 85 °C. The active ingredient, Nys, was added to the lipid phase and held for 15 min under stirring at the same temperature. Then, the lipid mixture was added to the aqueous phase, forming a pre-emulsion. The pre-emulsion was maintained under continuous stirring for 30 min at 85 °C, and then it was subjected for 2 min to high shear homogenization (HSH) at 10,000 rpm (Lab Homogenizer PRO250, 0–28,000 rpm, power of 300 W, Germany) and 5 min at 600 bar in a high-pressure homogenizer (HPH) (APV 2000 Lab Homogenizer, Germany). The formed emulsion was allowed to cool down at room temperature under continuous stirring to form a dispersion of the NLC loaded with Nys. The dispersion was freeze-dried in order to remove water by freezing for 24 h at –25 °C and then freeze drying for 3 days at –50 °C by using an Alpha 1-2 lyophilizer LD Freeze Drying System (Germany). The composition of the lipid carriers in the dispersion is shown in Table 1.

Table 1
The composition of NLC loaded with different amounts of nystatin.

Lipid phase in dispersion[a] (%)	Basil oil concentration in lipid matrix[b] (%)	Nystatin (%)			
		0	0.5	1	2
10	10	NLC 1	NLC 2	NLC 3	NLC 4
	20	NLC 5	NLC 6	NLC 7	NLC 8
	30	NLC 9	NLC 10	NLC 11	NLC 12
12	10	NLC 13	NLC 14	NLC 15	NLC 16
	20	NLC 17	NLC 18	NLC 19	NLC 20
	30	NLC 21	NLC 22	NLC 23	NLC 24

[a] Samples were synthetized with 2.5% (w/w) surfactant mixture, Tween 80:poloxamer:phosphatidylcholine in a 4.67:1:1 ratio.
[b] The lipid phase was composed of CP:GMS:BO with various concentrations of BO. The ratio CP:GMS was kept constant at 1:1.

2.3. Characterization of size, uniformity and stability of NLC

Using the Zetasizer Nano ZS apparatus (Malvern Instruments, Malvern, UK), particle sizes were determined by dynamic light scattering method (DLS). The conditions for measuring the mean particle size (Zave) and the polydispersity index (PdI) of the samples were as follows: scattering angle of 90° and temperature of 25 °C. To obtain the appropriate dispersion intensity, the samples were diluted with deionized water, and particle size evaluation was performed using the intensity distribution. Average diameters and polydispersity index of particles were obtained from an average of three measurements. Using the same apparatus, measurements of electrophoretic mobility of NLC into an electric field has been made based on the Helmholtz–Smoluchowski relationship in order to determine the zeta potential (ZP).

NLC dispersions were diluted with deionized water and the conductivity was adjusted to 50 mS/cm using a sodium chloride solution (0.9%, w/v). ZP is the average value of the measurements made in triplicate at 25 °C.

2.4. Transmission electronic microscopy

The morphology of NLC loaded with Nys was determined by using a transmission electron microscope (Philips 208 S, The Netherlands). Samples of the NLC in dispersion were diluted with ultrapure water in a ratio of 1:50. A drop of diluted solution was placed on a carbon-coated copper grid, and after 15 min the sample was photographed.

2.5. Percentage of nystatin loaded into NLC

The entrapement efficiency of Nys into NLC was evaluated using the UV absorbance at λ_{max} of Nys according to the Lambert–Beer law. The concentration of free Nys from NLC loaded with 0.5, 1 and 2% antibiotic was determined at λ_{max} = 305 nm. Samples were prepared by adding 0.03 g of lyophilized NLC–Nys in 10 mL of ethanol. The filtrate was exposed to UV–Vis spectroscopy (UV–VIS–NIR spectrophotometer type V570, Jasco) and analyzed using the calibration curve in the concentration range of 0.05 ÷ 2 g/L Nys, with a correlation coefficient R^2 = 0.9996. The percent of entrapement efficiency was calculated calculated using the following formula:

$$EE\% = \frac{C_{Nys\ \ initial} - C_{free\ \ Nys}}{C_{Nys\ \ initial}} \times 100 \quad (1)$$

2.6. Differential scanning calorimetry (DSC)

DSC analyzes the structural changes that appeared in the lipid matrix due to temperature variation. It is a technique used to obtain information about the physical and energy properties of the compounds or formulations. DSC analysis is useful to understand the interaction between the active compound and lipids, as well as between solid lipids and oils. DSC analysis was performed using a differential scanning calorimeter, Jupiter STA 449C (Netzsch). NLC samples (10 mg) were weighed in standard aluminum vessels and an empty vessel was used as a reference. The samples were heated with a temperature rate of 5 °C/min, in the range of 30–100 °C.

2.7. Antioxidant activity of nystatin loaded NLC

Antioxidants are molecules that interact with free radicals and break the chain reaction before damaging essential molecules [36]. The antioxidant activity represents the capacity of the system to scavenge the reactive oxygen species measured in vitro by a chemiluminometer Tuner Design TD 20/20, USA. A cyclic hydrazine (luminol) was used as a light amplifying substance, which emits light when it is oxidized and it is converted in an excited aminophtalate ion in the presence of oxidized species, such as superoxide, hydrogen peroxide, hydroxyl radical, free oxygen, and lipid peroxide radicals. The free radical generator system used was composed of luminol and hydrogen peroxide in buffer solutions of Tris–HCl (pH 8.6). The samples were prepared by adding 0.0015 g of lyophilized NLCs into 10 mL of dimethyl sulfoxide and subjecting them to ultrasonication for 3 min. The antioxidant activity (percentage of scavenged free radicals) of NLC was calculated using the relation:

$$\%AA = \frac{I_0 - I_s}{I_0} \times 100 \quad (2)$$

where I_0 is maximum chemiluminescence for the standard sample at t = 5 s, I_s is the maximum chemiluminescence of the sample at t = 5 s.

2.8. Antimicrobial activity

The antimicrobial activity of NLC was tested in vitro against human pathogenic microbes (pathogenic and conditionally pathogenic species). In order to determine the antifungal activity, the microbial strains used were *Candida albicans* ATCC 10231 and *Aspergillus niger* ATCC 15475. The antibacterial activity of the samples was tested by using *Escherichia coli* ATCC 8738.

Escherichia coli was grown in Luria Bertani Agar, LBA, plates at 37 °C with medium composition (M1): peptone, 10 g/L; yeast extract 5 g/L, NaCl 5 g/L and agar 20 g/L.

Candida albicans was grown in Malt Extract Agar, MEA, (Merck) with medium composition (M2): malt extract 17 g/L and agar 20 g/L. The mold *Aspergillus niger* was grown in Potato-Dextrose-Agar, PDA, (Merck) with medium composition (M3): potato infusion 4 g/L, dextrose 20 g/L and agar 15 g/L. The stock culture was maintained at 4 °C. The bacterial plates were incubated for 24 h at 37 °C while fungal and yeast plates were incubated for 48 h at 28 °C.

The assay was done using the agar well diffusion method [36]. Sterile agar plates were prepared by pouring the sterilized media in sterile Petri dishes under aseptic conditions. One millilitre of the test microorganism was spread on agar plates. Using a sterile Durham tube with a diameter of 6 mm, the wells were made according to the number of samples. The wells were inoculated with 50 μL of sample. The antimicrobial activity was interpreted based on the size of inhibition zone (IZ) diameter, which was measured in mm from observation of clear zones surrounding the wells. Each test was done in triplicate.

3. Results and discussion

3.1. Particle size and morphology of Nys–NLC

In order to obtain NLC with a higher loading capacity of the nystatin, the total amount of lipid mixture was increased from 10% to 12% in the aqueous dispersion (w/w). The influence of the basil oil amount on the particle size and loading capacity of the formulation was studied by varying the proportion of the oil from the lipid mixture by increasing its value from 1% to 3% (w/w of NLC in dispersion). The particle sizes of NLCs prepared with 12% lipids are greater than those of NLCs with 10% lipids. This effect could be due to an insufficient amount of surfactant in the case of carriers prepared with a higher concentration of the lipid mixture (Fig. 2).

In general, by increasing the basil oil concentration from 1 to 3%, the particle size of loaded NLC prepared with a content of 12% lipids was decreased owing to the lower viscosity (a better destruction of the emulsion droplets during the homogenization procedure) and a better solubility of lipophilic Nys in the lipid network. The incorporation of 0.5% Nys into NLC determines an initial reduction in the particles size of loaded nanocarriers as compared with those of free NLC. By further increasing the concentration of Nys to 1% and 2%, the particles sizes of the resulted NLCs are increasing, the NLC with 2% Nys presenting the largest particle sizes (e.g., 144 ÷ 178 nm).

The best results in terms of size and polydispersity index were obtained for NLC 22 and 23 prepared with 3% basil oil and loaded with 0.5 and 1% nystatin, respectively. In order to confirm the DLS measurements, TEM analysis was performed (Fig. 3). The developed NLC showed homogenous particles with spherical shape and diameters around 100 nm for NLC with 3% BO and 0.5% (NLC 22) and 1% Nys (NLC 23).

3.2. Stability of Nys–NLC aqueous dispersions

Zeta potential measurements on Nys–NLC showed a slight value variation (Fig. 4). In general, all NLC formulations are stable with ZP values less than −25 mV, which indicates a good stability of the aqueous dispersion and a low risk for Nys–NLC to aglomerate. It can be observed that by loading Nys into NLC leads to higher zeta potentials when compared to unloaded NLC. Some examples of electrokinetic potential distribution were shown in Fig. 5.

3.3. Stability over time of Nys–NLC

After preparation, the NLC aqueous dispersion was stored under refrigeration at 4 °C and monthly the particle size, PdI and zeta potential were examined during a period of two months. In general, all Nys–NLC proved to be stable during two months, with no particle agglomeration (Fig. 6). Significant variations in particle size, but with no major variations for PdI (data not shown), were noticed at two months for 1% and 2% Nys encapsulated into NLCs

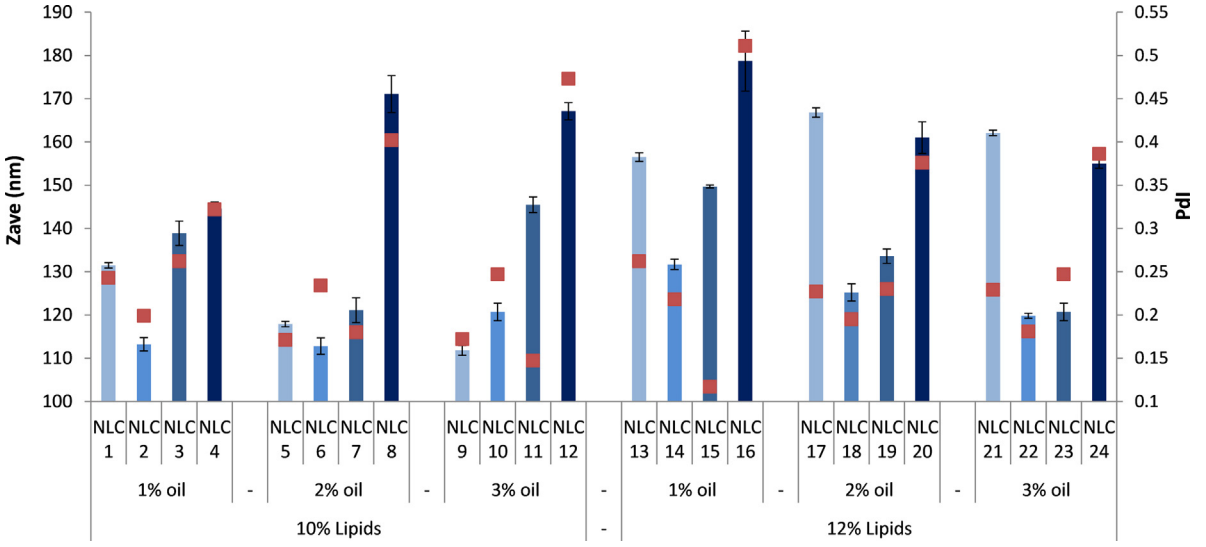

Fig. 2. (Color online.) Particle size (Zave) and polydispersity index (PdI) of free and Nys–NLC.

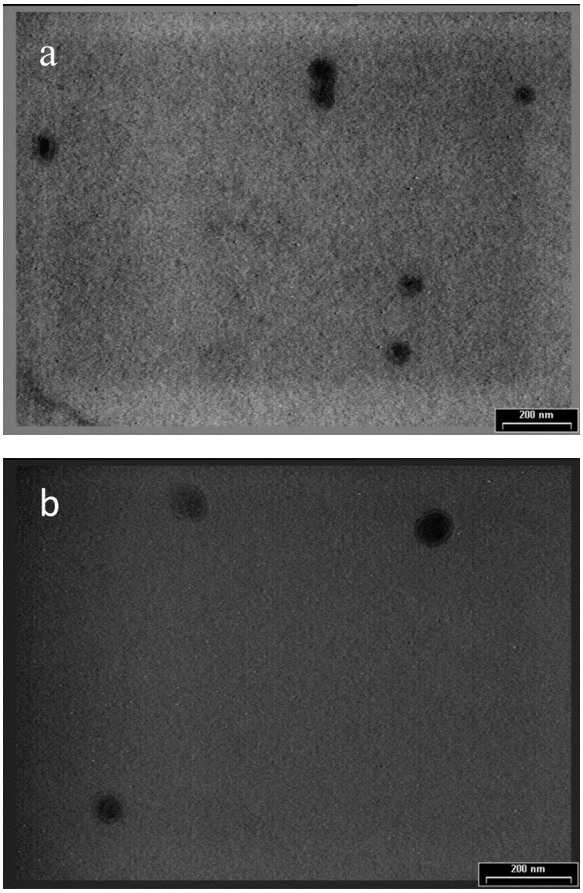

Fig. 3. TEM image for (a) NLC 22 and (b) NLC 23.

developed based on 12% lipids with different amounts of oils.

All NLC showed a slow zeta potential decrease during two months (Fig. 7), which demonstrates a good stability of the lipid nanocarriers in dispersion. Taking into consideration the variations in particle size of NLCs, it can be concluded that the electrostatic particle charge is not the single factor that can influence the formulation stability.

3.4. Entrapment efficiency of nystatin loaded into NLC

The entrapment efficiency of NLC with antibiotic was influenced by the Nys concentration used for encapsulation (Fig. 8). For instance, for both types of lipid matrix (prepared with 10% or 12% lipid mixtures) with 10% basil oil, a greater entrapment efficiency was obtained by encapsulating 2% nystatin. This behavior was not observed for the NLC prepared with 30% basil oil; in the latter case, a decrease in encapsulation efficiency is noticed. Also, by increasing the basil oil content in the lipid matrix from 1% to 3% led to an increased loading capacity of the lipid matrix, by creating an additional disorder among lipid chains that creates new spaces to better accommodate the antibiotic.

For NLC prepared with 12% lipids and loaded with various concentrations of Nys, the entrapement efficiency is lower than that for NLC prepared with a 10% lipid mixture. The explanation of this behavior could be attributed to the changes that occur within the lipid chains of the matrix and to the fact that the amount of surfactant per unit of lipids is less in the case of NLC with 12% lipids.

3.5. Structural arrangement of lipid matrix after Nys encapsulation

The changes in the crystalline lattice of Nys–NLC were analyzed by DSC. From Fig. 9, it can be seen that the melting point of the lipid matrix of NLC 5–7 is lower than that of the physical mixture (Fig. 9A). Also, lipid nanocarriers undergo a narrowing in the melting range and a decrease of the melting enthalpy as compared with physical mixtures. These observations are attributed to the presence of surfactants, which provides an ordered lipid arrangement, and to the small size of particles, which determines an increase in the specific surface area. The formation of nystatin loaded lipid nanocarriers with a melting temperature higher than the body temperature is confirmed.

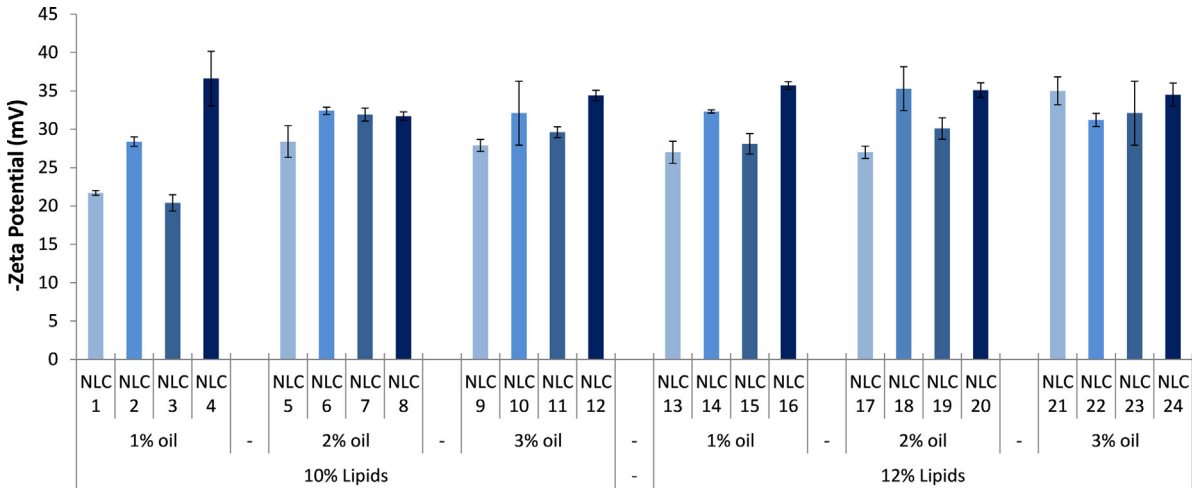

Fig. 4. (Color online.) Stability evaluation in terms of zeta potential (ZP) of free and Nys–NLC.

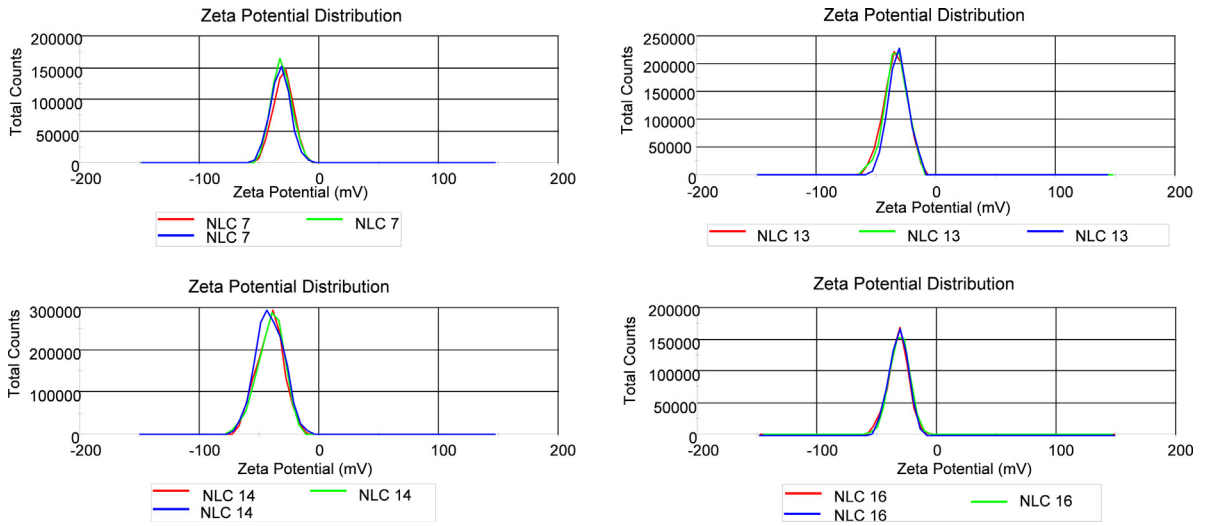

Fig. 5. (Color online.) Examples of electrokinetic potential distribution of free and Nys–NLC.

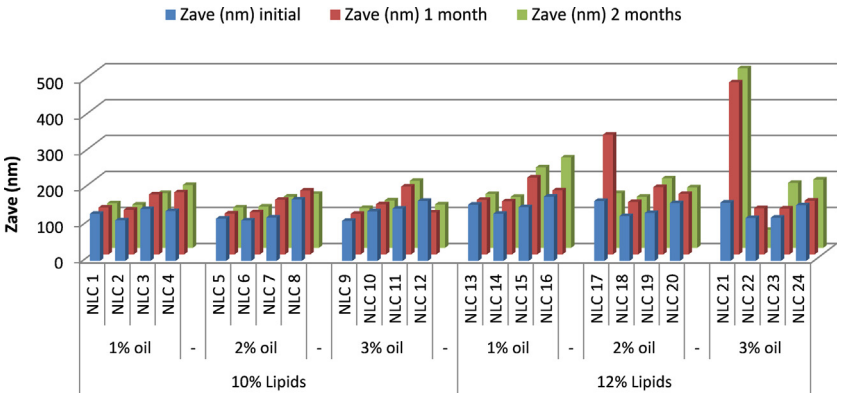

Fig. 6. (Color online.) Stability over time in terms of particle size of free and Nys–NLC.

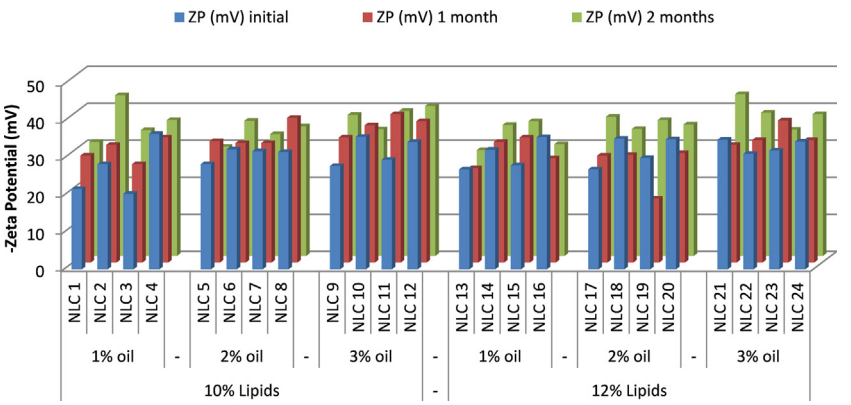

Fig. 7. (Color online.) Stability over time in terms of ZP of free and Nys–NLC.

As expected, the presence of the basil oil inside the nanostructured carriers results in a disordered lipid matrix with many imperfections, as confirmed by the DSC curves. By observing the calorimetric curve, there is a decrease in the intensity of the endothermic peak and in the melting temperature of NLC as the amount of oil was increased (Fig. 9B). A NLC lipid matrix consisting of 12% lipids shows a melting point and an enthalpy higher than those of a NLC with 10% lipids, and thus a larger particle size for NLC prepared with 12% lipids [confirmed by DLS analysis, (Fig. 9C)]. Thus, it can be assumed that an efficient rearrangement of the liquid and solid lipids, associated

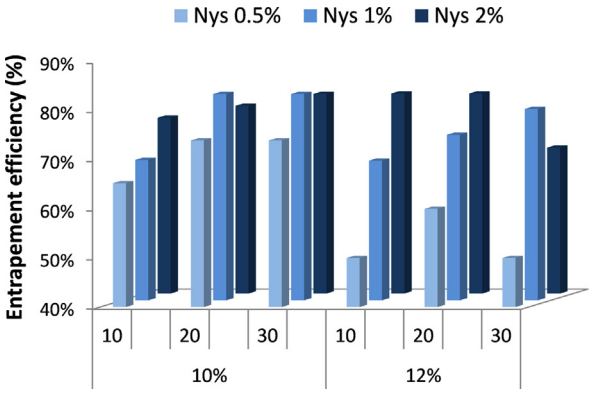

Fig. 8. (Color online.) Entrapment efficiency (EE%) depending on the concentration of Nys.

with a more homogeneous lipid core, occurred after Nys encapsulation into the lipid nanocarriers.

In general, the encapsulation of 1% Nys into NLC with 10% and 30% BO causes a slight increase in the melting enthalpy, suggesting a more ordered matrix with a greater expulsion capacity, while 1% Nys–NLC with 20% BO shows a lower melting enthalpy and higher encapsulation efficiency when compared to 0.5% Nys–NLC. Thus, the concentration of 20% BO is optimal to obtain NLC with appropriate disorder to provide a good encapsulation efficiency for 1% Nys.

3.6. In vitro evaluation of antioxidant activity of Nys–NLCs

In order to determine the antioxidant activity of Nys–NLC formulations, Nys–NLC, free NLC and basil oil were

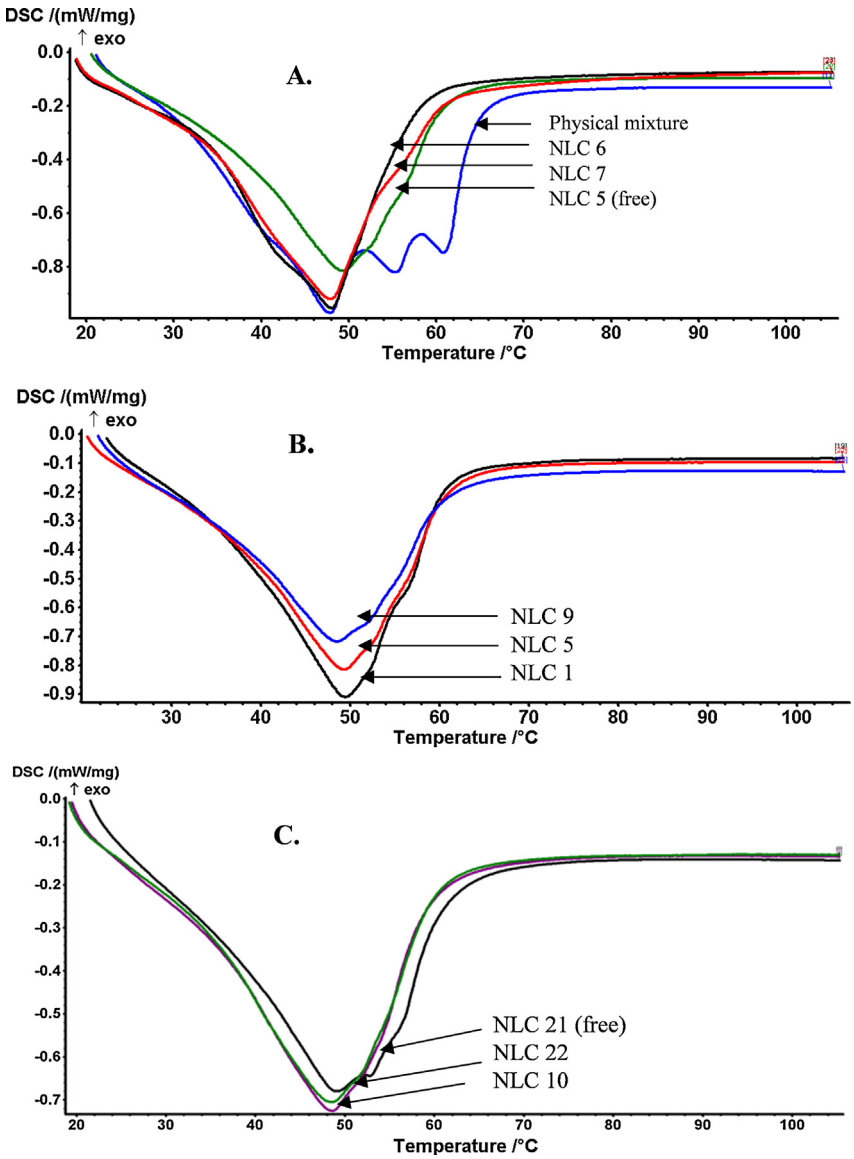

Fig. 9. (Color online.) The differential calorimetry curves for NLCs loaded with Nys.

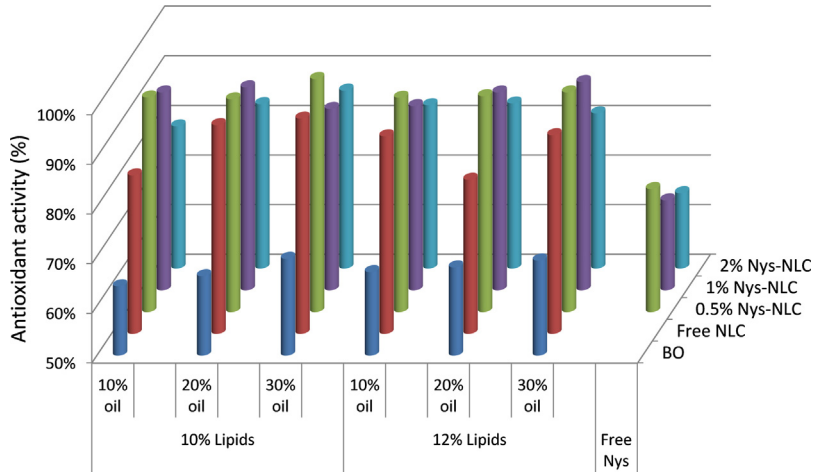

Fig. 10. (Color online.) Comparative antioxidant activity of native basil oily extract and NLC prepared with 10% and 12% lipid mixture and loaded with 0%, 0.5%, 1% and 2% Nys.

exposed to a free radical generating system. Free NLCs present a great antioxidant activity (83 ÷ 93%), which might be associated with the fact that the basil oil has the ability to develop a chain reaction lock. Both active principles used in NLC synthesis, Nys and basil oil, demonstrate an effective antioxidant activity (e.g., 69% for BO and 74% for Nys) (Fig. 10).

For most nanocarriers loaded with Nys, the antioxidant activity was maintained in the area of a high ability to scavenge free radicals. The best results in terms of AA% were obtained by encapsulation 0.5% Nys (e.g., AA = 93 ÷ 96% for NLC 2, 6, 10 and 93 ÷ 94% for NLC 14, 18, 28). The explanation for this behavior could be due to the synergistic effect of basil oil and Nys brought to

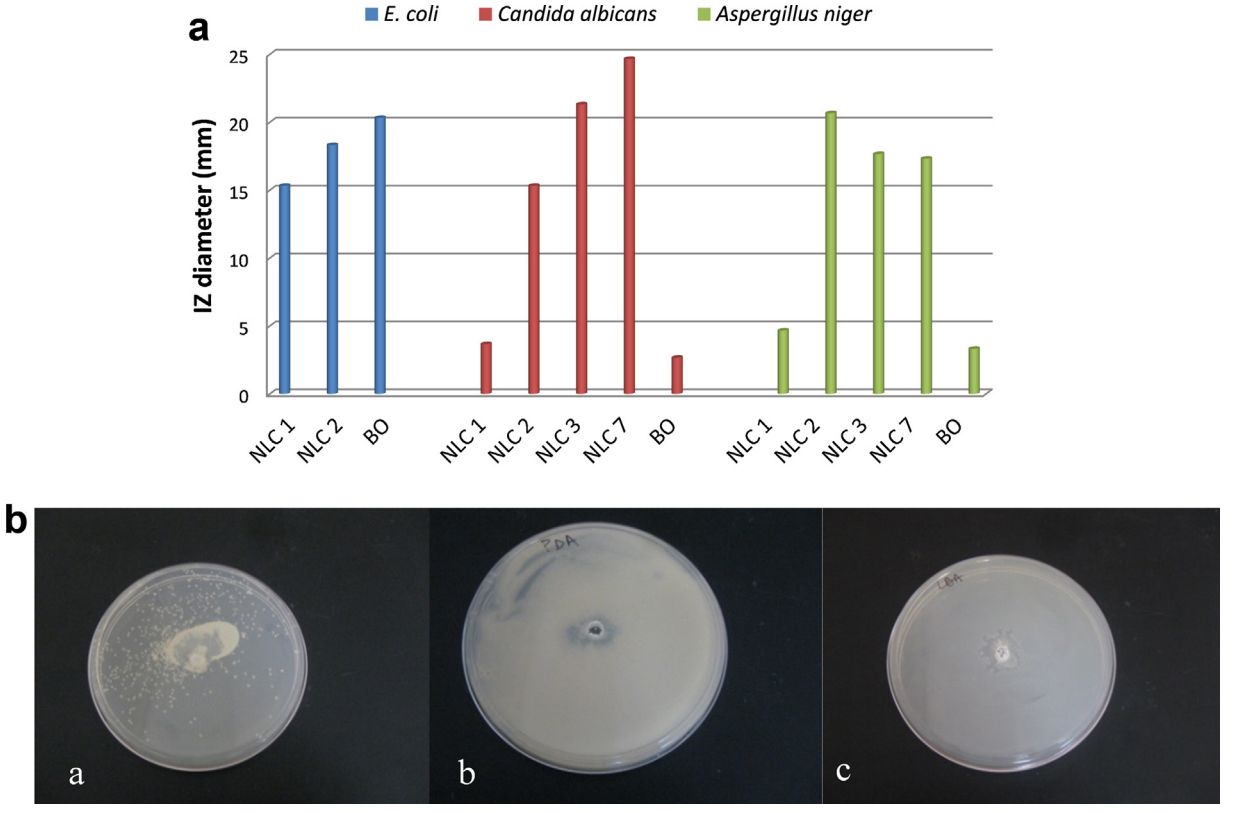

Fig. 11. (Color online.) In vitro antimicrobial activity of NLCs against various human pathogenic species. A. Inhibition zone (IZ) diameter. B. Images of Petri dishes of various NLCs formulations: (a) NLC 7 against *Candida albicans*, (b) NLC 2 against *Aspergillus niger*, (c) NLC 2 against *Echerichia coli*.

nanometer size. By increasing the basil oil amount, a slow enhancement of antioxidant activity was observed. On the other hand, the antioxidant activity of Nys–NLC was decreased by encapsulating high concentrations of Nys (e.g., 2% antibiotic).

3.7. In vitro determination of atimicrobial activity of Nys–NLCs

The developed NLC were tested in order to evaluate their properties to combat infections caused by certain microorganisms. Three kinds of microorganisms, *C. albicans* ATCC 10231, *A. niger* ATCC 15475 and *E. coli* ATCC 8738 were selected taking into consideration the caused infections. The antimicrobial activity of lipid nanocarriers with various concentrations of antibiotic and basil oil is comparatively presented in Fig. 11. Among the tested samples, NLC 7 based on 2% BO loaded with 1% Nys provided the best activity against microorganisms type *C. albicans* ATCC 10231, with an inhibition zone of 24.7 mm. For NLC 3 based on 1% BO the anti-*Candida* activity remains satisfactory, but the inhibition zone diameter decreased by 21.3 mm, suggesting that the basil oil extract has itself a mild antifungal activity. The encapsulation of a lower Nys concentration (e.g., 0.5%, NLC 2) led to a significant reduction in the antifungal activity, but it still remains in the area of antimicrobial activity (IZ diameter of 15.3 mm). Free NLC showed poor anti-*Candida* activity (e.g., IZ diameter of 3.7 mm).

As reffering to the antifungal activity of nanocarriers loaded with Nys *against A. niger* ATCC 15475, worthy results were observed (Fig. 11A). The free nanocarriers exibit a low antimicrobial activity (e.g., IZ diameter of 4.7 mm), while loading them with 0.5% and 1% nystatin results in obtaining an effective antifungal activity (e.g., IZ = 20.2 mm for NLC 2 and 17.5 mm for NLC 3). These data indicate that the antibiotic is mainly responsible for the anti-*Candida* and antifungal activity and the basil oil extract has a small contribution (the native basil oil extract samples showed a weak antimycotic activity).

Testing the nanocarriers against *E. coli* ATCC 8738 highlighted an appropriate antimicrobial activity for both free NLC and native basil oil. However, the loading of 0.5% Nys into NLC has resulted in a slight increase of the IZ diameter (e.g., 15.3 mm for NLC 1 and 18.3 for NLC 2). The superior activity of basil oil extract against *E. coli* (IZ diameter of 20.3 mm) is attributed to their antimicrobial activity, fact that is supported by the literature [12,18,19].

4. Conclusions

The exploitation of vegetable oils with biological effectiveness for obtaining lipid nanocarriers with targeted properties represents an alternative to conventional liquid lipids, e.g., oleic acid, medium chain triglycerides. Nanostructured carriers based on a blend of basil oil extract and solid lipids were successfully prepared in the present paper as an appropriate encapsulation system for nystatin. Formulation factors, such as the concentration of the basil oil extract, the concentration of the lipid phase in the aqueous dispersion, and the nystatin loading were evaluated to produce lipid based nanocarriers with enhanced antifungal and antioxidant activity.

The NLCs developed with oily plant extract have proved an effective entrapping capacity of nystatin, an encapsulation efficiency reaching 82% as the basil oil content was increased from 1 to 3%. Both active ingredients used, nystatin and basil oil, have resulted in the development of effective NLCs that manifest the capacity to capture the free oxygen radicals, with antioxidant activity ranging between 93 and 96%.

Among the synthesized lipid nanocarriers, several of them have proven their ability to exhibit remarkable in vitro antimicrobial activity against three tested strains, e.g., *C. albicans*, *A. niger*, and *E. coli*, the inhibition zone being influenced by the antibiotic concentration and type of microorganisms. The lipid nanocarriers based on 2% basil oil and loaded with 1% Nys was found to be the most active against *C. albicans*.

Acknowledgements

This work was funded by the Sectorial Operational Program Human Resources Development 2007–2013 of the Romanian Ministry of Labor, Family and Social Protection, by financial agreements POSDRU/107/1.5/S/76903. This research was also supported by a grant of the Ministry National Education, CNCS – UEFISCDI, Romania, project number PCE_PN-II-ID-PCE-2012-4-0111.

References

[1] J. Guarro, J. Gené, A.M. Stchigel, Clin. Microbiol. Rev. 12 (1999) 454.
[2] M.A. Pfaller, D.J. Diekema, Clin. Microbiol. Rev. 20 (2007) 133.
[3] R.H. Roda, M. Young, J. Timpone, J. Rosen, Diagn. Microbiol. Infec. Dis 63 (2009) 96.
[4] M. Klepser, J. Crit. Care 26 (2011) 225e1.
[5] D.M. Burton, A.B. Seid, D.B. Kearns, S.M. Pransky, Int. J. Pediatr. Otorhinolaryngol. 23 (1992) 171.
[6] G.P. Bodey, Am. J. Med. 81 (1986) S11.
[7] D.K. Stein, A.M. Sugar, Diagn. Microbiol. Infec. Dis. 12 (1989) S221.
[8] S. Sciascia, M.J. Cuadrado, M.Y. Karim, Best. Pract. Res. 27 (2013) 377.
[9] T. Valkovic, A.D. Nacinovic, D. Petranovic, Med. Hypotheses 81 (2013) 1137.
[10] K. Peter, Linden, Infect. Dis. Clin. N. Am. 23 (2009) 535.
[11] A.J. Huh, Y.J. Kwon, J. Control Release 156 (2) (2011) 128.
[12] S. Güngör, M.S. Erdal, B. Aksu, JCDSA 3 (2013) 56.
[13] H.R. Ashbee, M.H. Gilleece, in: S. Padmanabhan (Ed.), Handbook of Pharmacogenomics and Stratified Medicine, Academic Press (Elsevier Inc), 2014, p. 879.
[14] A.-M. Manea, B.S. Vasile, A. Meghea, C. R. Chimie 17 (2014) 331.
[15] M. Zuzarte, M.J. Gonçalves, C. Cavaleiro, M.T. Cruz, A. Benzarti, B. Marongiu, A. Maxia, A. Piras, L. Salgueiro, Ind. Crop. Prod. 44 (2013) 97.
[16] I. Rasooli, M.R. Abyaneh, Food Control 15 (2004) 479.
[17] S.D. Kocic-Tanackov, G.R. Dimic, L.V. Mojović, J.D. Pejin, I.J. Tanackov, Food Sci. Technol. 59 (2014) 426.
[18] H. Mighri, H. Hajlaoui, A. Akrout, H. Najjaa, M. Neffati, C. R. Chimie 13 (2010) 380.
[19] R. Semis, S.S. Nili, A. Munitz, Z. Zaslavsky, I. Polacheck, E. Segal, J. Antimicrob. Chemother. 67 (2012) 1716.
[20] S. Pál, S. Nagy, T. Bozó, B. Kocsis, A. Dévay, Eur. J. Pharm. Sci. 49 (2013) 258.
[21] M.E. Barbinta-Patrascu, I.-R. Bunghez, S.M. Iordache, N. Badea, R.-C. Fierascu, R.M. Ion, J. Nanosci. Nanotechnol. 13 (2013) 2051.
[22] I. Lacatusu, N. Badea, D. Bojin, S. Iosub, A. Meghea, J. Sol-Gel Sci. Technol. 51 (2009) 84.
[23] I. Lacatusu, N. Badea, R. Nita, M. Giurginca, D. Bojin, S. Iosub, A. Meghea, J. Phys. Org. Chem. 22 (2009) 1015.
[24] M.E. Barbinta-Patrascu, L. Tugulea, I. Lacatusu, A. Meghea, Mol. Cryst. Liq. Cryst. 522 (2010) 148.

[25] I. Lacatusu, N. Badea, O. Oprea, D. Bojin, A. Meghea, I. Lacatusu, N. Badea, Soft Mater. 11 (2013) 75.
[26] F. Li, Y. Weng, L. Wang, H. He, J. Yang, X. Tang, Int. J. Pharm. 393 (2010) 203.
[27] J. Tomasina, S. Lheureux, P. Gauduchon, S. Rault, A. Malzert-Fréon, Biomaterials 34 (2013) 1073.
[28] C.W. How, A. Rasedee, S. Manickam, R. Rosli, Colloids Surf. B Biointerf. 112 (2013) 393.
[29] G. Niculae, N. Badea, A. Meghea, O. Oprea, I. Lacatusu, Photochem. Photobiol. 89 (2013) 1085.
[30] G. Niculae, I. Lacatusu, A. Bors, R. Stan, C.R. Chimie 17 (2014) 1028.
[31] F. Tamjidi, M. Shahedi, J. Varshosaz, A. Nasirpour, Innov. Food Sci. Emerg. 19 (2013) 29.
[32] G. Niculae, I. Lacatusu, N. Badea, R. Stan, B.S. Vasile, A. Meghea, Photochem. Photobiol. Sci. 13 (2014) 703.
[33] J. Pardeike, A. Hommoss, R.H. Müller, Int. J. Pharm 366 (2009) 170.
[34] E.B. Souto, A.J. Almeida, R.H. Müller, J. Biomed. Nanotechnol. 3 (2007) 317.
[35] I. Lacatusu, G. Niculae, N. Badea, R. Stan, O. Popa, O. Oprea, A. Meghea, Chem. Eng. J. 246 (2014) 311.
[36] M.E. Barbinta-Patrascu, C. Ungureanu, S.M. Iordache, A.M. Iordache, I.-R. Bunghez, M. Ghiurea, N. Badea, R.-C. Fierascu, I Stamatin, Mat. Sci. Eng. C-Mater. 39 (2014) 177.